

IR Spectroscopic Study of H₂O₂, HDO₂, and D₂O₂ Isolated in Ar, Kr, and Xe MatricesMika Pettersson,^{*,†} Susanna Tuominen,[‡] and Markku Räsänen[§]

Laboratory of Physical Chemistry, P.O. Box 55, FIN-00014, University of Helsinki, Finland

Received: September 25, 1996; In Final Form: November 6, 1996[⊗]

The vibrational spectrum of hydrogen peroxide, released from an urea hydrogen peroxide adduct compound, is studied in Ar, Kr, and Xe matrices. The gaseous products of the thermal decomposition of urea hydrogen peroxide in an argon atmosphere are determined using a low-resolution fast scanning FTIR–gas analyzer. Upon the solid sample being warmed to temperatures of ~90 °C, only hydrogen peroxide is detected, and above that, NH₃ and HNCO are evolved due to the decomposition of urea. The hydrogen peroxide–rare gas matrices are prepared from urea hydrogen peroxide by sweeping Ar, Kr, or Xe gas over the solid sample kept at a suitable temperature. The ratio between trapped monomer and multimers can be controlled by varying the amount and the temperature of the sample and the gas flow rate. The results show that urea hydrogen peroxide is a convenient source of pure hydrogen peroxide for spectroscopic studies. The IR spectra of H₂O₂, HDO₂, and D₂O₂ in argon matrices are presented and compared with previous results. The krypton and xenon spectra are presented for the first time. Many of the peaks show a well-resolved doublet structure.

1. Introduction

Hydrogen peroxide is a molecule of considerable interest in many fields including atmospheric chemistry,¹ oxidation reactions,² and photodissociation dynamics.^{3–8} Handling of pure hydrogen peroxide requires special techniques and care because of the danger of explosion.⁹ For chemical reactions, commercially available urea hydrogen peroxide (CO(NH₂)₂·H₂O₂) (UHP) has often been used as a source of hydrogen peroxide because it is much safer to use than pure H₂O₂.¹⁰

Thermal decomposition of UHP has been investigated by thermogravimetric methods, and it has been found^{11,12} that hydrogen peroxide is released first from the complex and further warming then results in a decomposition of urea. In this paper we show that quite pure hydrogen peroxide can be obtained from UHP without any significant decomposition to water and oxygen.

The IR spectrum of hydrogen peroxide is well-known in the gas phase^{13–18} and it has also been studied in nitrogen and argon matrices to some extent.^{19,20} The complexes between H₂O₂ and CO have been studied in solid O₂.²¹ In addition, photochemical reactions between H₂O₂ and C₂H₄ have been studied in an argon matrix.²² In this work we reexamine the infrared spectrum of H₂O₂ trapped in an argon matrix and extend these studies to krypton and xenon matrices. This paper is the first part of our studies of photochemical processes of H₂O₂ and its complexes in solid rare gas matrices. Another purpose of this study is to report a safe and convenient method for obtaining pure hydrogen peroxide for spectroscopic studies.

2. Experimental Section

2A. Gas Phase Measurements. The gas phase measurements were carried out using a previously described setup.²³ For thermal emission studies of UHP approximately 100 mg of the solid sample (Aldrich, 98% purity) was placed in a pyrex glass tube, which was held in a furnace. One end of the tube was connected to the multipass gas cell of the FTIR spectrometer (GASMET, Temet Instruments, Finland) with a 1/4 in. stainless

steel tube, and carrier gas was provided from the other end. Sample temperature was measured with a Fe–CuNi thermocouple, and the temperature was raised at an average rate of about 1.7 °C/min.

The spectra were recorded with the FTIR spectrometer designed originally for quantitative analysis of gas mixtures.²⁴ The flowing gas was led through the multipass gas cell (optical path length 1.5 m). The scanning rate of 12 scans/s (8 cm⁻¹ resolution) allowed us to monitor the changes in the gas concentrations practically in real time. For the background, 240 scans were coadded, and the spectra were measured by coadding 120 scans.

Argon (99.9%) was led through the gas handling system at room temperature until water vapor released from the walls could not be seen in the spectrum. The flow rate of the gas was not measured. After the system was stabilized at room temperature, the background spectrum was recorded and the sample spectra were recorded up to 143 °C in temperature intervals of ~3 °C.

2B. Matrix Isolation. Deposition of H₂O₂ emitted from UHP was performed by flushing UHP at selected temperature with the matrix gas. The deposition line was constructed from PFA plastic (Svigelok) in order to reduce the catalytic decomposition of hydrogen peroxide on the surfaces.²⁵ The gas line was constructed mainly from 1/4 in. tube. For technical reasons, we were forced to use a 10 cm long piece of 1/16 in. stainless steel capillary at the cryostat end of the system. Matrix gas was provided from a glass vacuum line, and the purity of the gases was 99.999% for Ar and 99.997% for Kr and Xe.

Typically 2–18 mg of the UHP sample was used in the experiments. The absolute concentration of hydrogen peroxide could not be determined, but its relative concentration could be varied by changing the deposition rate and/or temperature and/or the amount of the sample. However, it is possible to calculate the lower limits of the ratio between rare gas and H₂O₂ by calculating the amount of H₂O₂ in the sample and the amount of the deposited gas. By using a typical total amount of rare gas of 7 mmol and assuming the maximal H₂O₂ content in UHP, we obtain the lower limits for M/A ratios of 37 and 329 for 18 and 2 mg of UHP, respectively. The true values are probably much larger than these due to incomplete decomposition of UHP. To obtain matrices with a high monomer content it was

[†] E-mail: mika.pettersson@csc.fi.

[‡] E-mail: susanna.tuominen@csc.fi.

[§] E-mail: markku.rasanen@csc.fi.

[⊗] Abstract published in *Advance ACS Abstracts*, January 15, 1997.

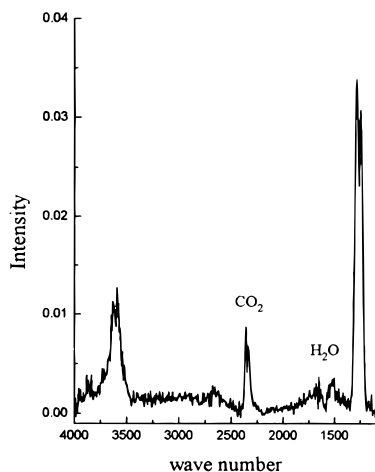


Figure 1. FTIR spectrum of gaseous hydrogen peroxide. Temperature of the UHP sample was 67 °C at the moment of measurement. The resolution is 8 cm⁻¹. CO₂ and water are indicated in the picture.

necessary to use only a few milligrams of UHP, kept at temperatures between 20 and 55 °C while flushing it with the matrix gas. The average deposition rate was 9.4 mmol/h of the matrix gas.

A closed cycle helium cryostat (Displex CS-202) providing temperatures down to 15 K was used in the experiments. The gas mixture was deposited onto a CsI window. The temperature was measured with a silicon diode (accuracy 0.5 K), and a resistive heater was used for obtaining higher temperatures. The spectra were recorded with a Nicolet 60 SX FTIR spectrometer. A resolution of 1 or 0.25 cm⁻¹ was used and 200 scans were averaged.

The deuterated peroxides were obtained from deuterated UHP synthesized by simply mixing D₂O and a 30% water solution of hydrogen peroxide and urea, heating the mixture up to 60 °C, and pumping the water off in vacuum.²⁶

3. Results

3A. Gas Phase Analysis. Only hydrogen peroxide and a small amount of water is seen in the spectrum recorded when heating the UHP sample up to 92 °C. This is close to the value of 85 °C given by Ball and Massey¹² for the highest temperature at which H₂O₂ is the only species released from UHP. Above 92 °C, NH₃ and HNCO, which are the decomposition products of urea,²⁷ are detected. HNCO was identified on the basis of the unresolved bands at 3535 and at 2269 cm⁻¹ (lit.^{28/3531} and 2274 cm⁻¹). The slight discrepancy between our uppermost temperature for H₂O₂ release and that of Ball and Massey may in part be explained by the time taken to replace the gas cell volume of 1.5 L.

A typical low-resolution spectrum of the flowing gas is displayed in Figure 1. The temperature of the sample at the moment of recording the spectrum was 67 °C. The fundamentals of H₂O₂ clearly dominate the spectrum. The broad 3600 cm⁻¹ band includes both the symmetric and antisymmetric stretchings, and the 1260 cm⁻¹ band is due to the antisymmetric bending mode. The band at 2345 cm⁻¹ is due to residual CO₂ in the spectrometer despite purging of the device. Water vapor can barely be seen in the 1600 cm⁻¹ region. This demonstrates that only a minor fraction of hydrogen peroxide is decomposed during its passage from the sample tube to the gas cell and during the time it spends in the cell. For the matrix isolation experiments, this observation is of great value because it allows us to use UHP as a precursor of hydrogen peroxide.

3B. Matrix Isolation. A survey spectrum of H₂O₂ isolated in solid Ar is displayed in Figure 2. The peaks belonging to

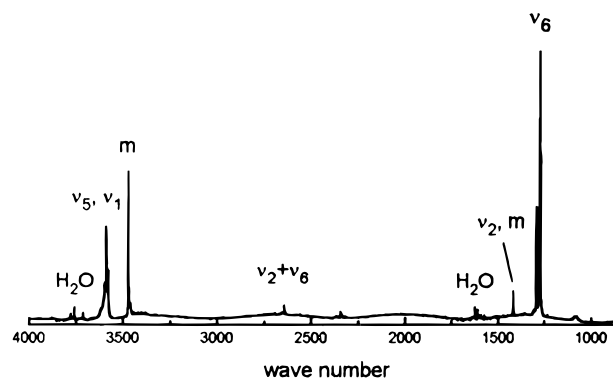


Figure 2. Survey spectrum of H₂O₂ isolated in an argon matrix. Impurity water peaks are indicated in the picture. Multimetric absorptions are marked with m. The resolution is 1.0 cm⁻¹.

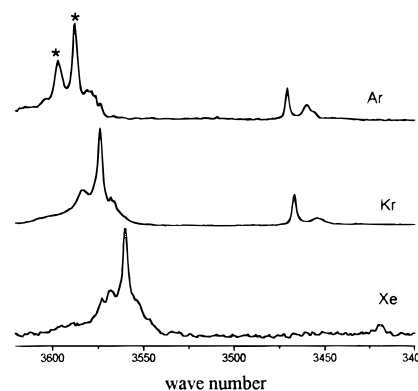


Figure 3. OH stretching region of matrix isolated H₂O₂. Monomeric absorptions are marked with an asterisk in the argon spectrum. The resolution is 1.0 cm⁻¹.

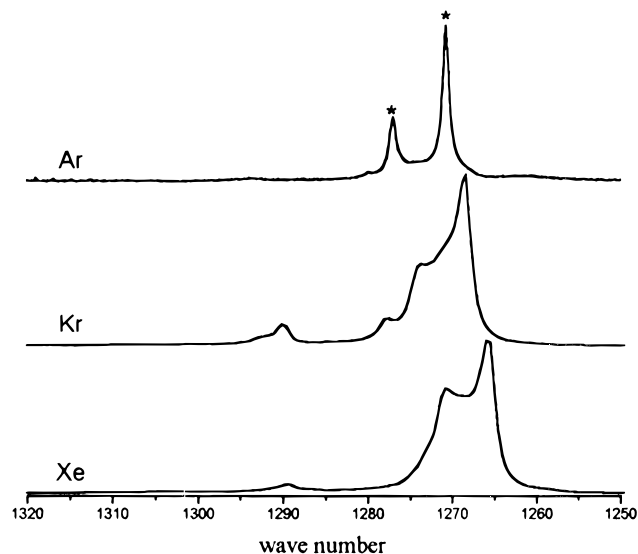


Figure 4. Bending region of matrix isolated H₂O₂. Monomeric absorptions are marked with an asterisk in the argon spectrum. The resolution is 1.0 cm⁻¹, except in argon spectrum, which is recorded with a resolution of 0.25 cm⁻¹.

water are indicated, and clearly, large quantities of hydrogen peroxide can be deposited without significant contamination by water. The water peaks present all belong to the monomer,²⁹ which eliminates the possible overlap of the H₂O₂ bands with water. In this sample the concentration of H₂O₂ was the highest of all experiments which resulted in strong multimer peaks.

Figures 3 and 4 display the stretching and bending regions of H₂O₂ in Ar, Kr, and Xe matrices. The concentration and monomer/multimer ratio vary in the different matrices. How-

TABLE 1: Wave Numbers of the Peroxides in an Argon Matrix. The Two Components of the Resolved Double-Minimum Doublets in Bold

H ₂ O ₂ (cm ⁻¹)	HDO ₂ (cm ⁻¹)	D ₂ O ₂ (cm ⁻¹)	assignment
3597.0		2655.7 ^a	ν_5, ν_1^b
3587.8		2651.3 ^a	ν_5, ν_1
		2645.3 ^a	ν_5, ν_1
3587.5		2647.2 ^a	N ₂ complex
	3587.3		OH stretching, possibly multimer
3587.7		2638.5 ^a	dimer/multimer
3581.0		2635.8 ^a	dimer/multimer
3576.4			dimer/multimer
3470.7	3470.1	2564.4 ^a	dimer/multimer
3460.0	3456.0	2554.2 ^a	dimer/multimer
	3454.7	2541.9 ^a	dimer/multimer
2695.0			$\nu_2 + \nu_6$, dimer/multimer
2653.0		1974.2	$\nu_2 + \nu_6$
2643.6		1965.2	$\nu_2 + \nu_6$
2560.3			dimer/multimer
1417.9			ν_2 , dimer/multimer
	1350.3		OH bending
	1346.4		dimer/multimer
	1342.6		OH bending
1293.2		965.0	dimer/multimer
		962.9	dimer/multimer
		960.5	dimer/multimer
1279.9	992.2	955.8	N ₂ complex
1277.0			ν_6
1270.9		951.3	ν_6
	980.9		OD bending
869.3			ν_3 , dimer/multimer
865.6			ν_3 , dimer/multimer

^a HDO₂ and D₂O₂ absorptions could not be separated. ^b See discussion for the assignments of ν_5 and ν_1 .

ever, the spectra look very similar and the main difference is a normal shift to lower wavenumbers in the heavier rare gases. It is to be noted that under our sample preparation conditions we never saw any indication of urea or of its decomposition products in the matrix spectra. The observed absorptions for H₂O₂ and its deuterated analogues in different matrices are collected in Tables 1–3. A few bands were assigned to a hydrogen peroxide–N₂ complex. These peaks were observed only in matrices that also contained the water–N₂ complex peaks,³⁰ indicating a leak in the system. This complex was not studied systematically.

The peaks belonging to multimeric species could be separated from the monomer peaks by preparing matrices with different concentrations of H₂O₂. In the most diluted argon matrix only two bands remained in the OH stretching region at 3597.0 cm⁻¹ and 3587.8 cm⁻¹. In going to smaller M/A-ratios, the peaks at 3581.0, 3576.4, 3470.7, and 3460.0 cm⁻¹ increased their intensity and they are assigned to multimeric forms. The concentration studies also revealed that there must be a multimer peak overlapping with the 3587.8 cm⁻¹ absorption, because when multimers were present, its strength relative to the other monomer peak at 3597.0 cm⁻¹ was larger than that in monomeric matrices.

The multimeric peaks in the bending region could also be assigned according to the differences in the spectra at different M/A ratios. The most prominent observation in monomeric matrices is the doublet structure of the ν_6 bending fundamental (see Figure 4). In argon, these components occur at 1270.9 and at 1277.0 cm⁻¹.

We also observed the much weaker ν_3 (O–O stretching), ν_2 (symmetric bending), and $\nu_2 + \nu_6$ combination peaks at, respectively, 865.6, 1417.9, and 2643.6 cm⁻¹ (with a weaker component at 2653.0 cm⁻¹) in argon matrices. By comparing

TABLE 2: Wave Numbers of the Peroxides in a Krypton Matrix. The Two Components of the Resolved Double-Minimum Doublets in Bold

H ₂ O ₂ (cm ⁻¹)	HDO ₂ (cm ⁻¹)	D ₂ O ₂ (cm ⁻¹)	assignment
3583.6		2645.2	ν_1, ν_5^a
3574.0			ν_1, ν_5
	3573.3		OH stretching
	2640.6		OD stretching
	2635.8		OD stretching
3568.2		2638.6	dimer/multimer
3466.9	3451.8	2561.6	dimer/multimer
3454.9		2553.0	dimer/multimer
2649.7			$\nu_2 + \nu_6$
2636.3		1960.0	$\nu_2 + \nu_6$
1411.7			ν_2 , dimer/multimer
	1346.4		OH bending
	1342.1		dimer/multimer
	1339.6		OH bending
1290.1	989.9	963.8	dimer/multimer
		960.6	dimer/multimer
		958.1	dimer/multimer
		954.0	N ₂ complex
1277.7			ν_6
1273.7			dimer/multimer
1270.8			dimer/multimer
1268.7		949.9	ν_6
	978.7		OD bending
865.0			ν_3 , dimer/multimer
862.7			ν_3 , dimer/multimer

^a See discussion for the assignments of ν_1 and ν_5 .

TABLE 3: Wave Numbers of the Peroxides in a Xenon Matrix. The Two Components of the Resolved Double-Minimum Doublets in Bold

H ₂ O ₂ (cm ⁻¹)	HDO ₂ (cm ⁻¹)	D ₂ O ₂ (cm ⁻¹)	assignment
3573.3		2639	ν_1, ν_5^a
3568.0		2633.2	ν_1, ν_5
3560.0		2628.4	ν_1, ν_5
3559		2624.4	dimer/multimer
	3559.3		OH stretching
	2631.1		OD stretching
3419.9			dimer/multimer
		2533.1	dimer/multimer
		2529.2	
2644.0			$\nu_2 + \nu_6$
2639.6		1954.3	$\nu_2 + \nu_6$
2628.5			OH bending
	1341.8		dimer/multimer
	1339.6 sh		dimer/multimer
	1336.6		OH bending
1289.5	985.4	968.1	dimer/multimer
		961.8	dimer/multimer
1270.3			ν_6
1265.7		947.8	ν_6
	976.0		OD bending

^a See discussion for the assignments of ν_1 and ν_5 .

several spectra with different monomer/multimer ratio these values for ν_3 and ν_2 are assigned to multimeric forms.

In preparing the deuterated samples, we found that quite high degree's of deuteration could be achieved but that also HD and HH forms were present. Figures 5 and 6 display the bending absorptions of the deuterated forms. The ν_2 -bending mode, which is very weak in H₂ and D₂ forms, becomes intense in the antisymmetrical HD form, and in consequence, both of the OH and OD bending modes are observed for the HD form.

The OD stretching region shown in Figure 7 is more problematic than the others because ν_1 and ν_5 of D₂O₂ and OD stretching of HDO₂ all contribute to the observed absorptions. In addition, the splitting and the possibility of several different

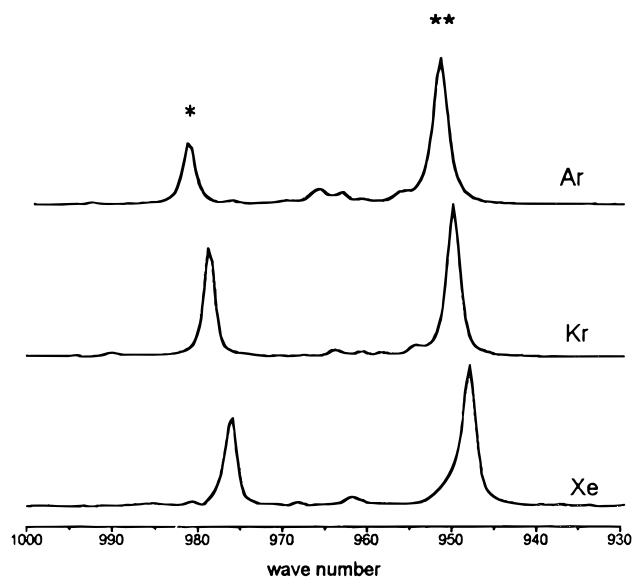


Figure 5. OD bending region of matrix-isolated HDO₂ and D₂O₂. Monomeric HDO₂ is marked with * and monomeric D₂O₂ marked with **. The resolution is 1.0 cm⁻¹.

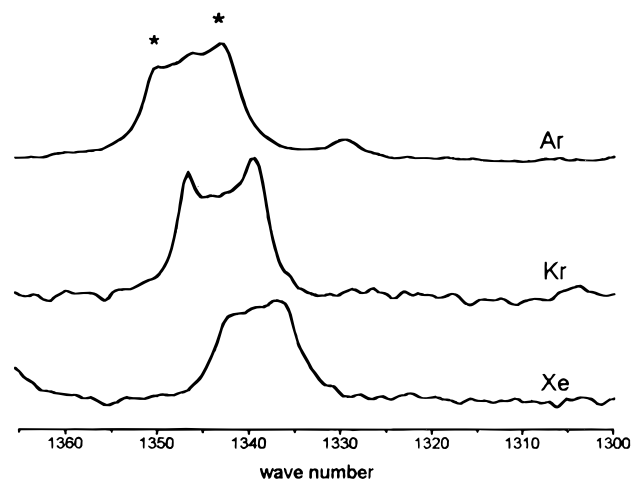


Figure 6. OH bending region of HDO₂. Monomeric absorptions are marked with * in the argon spectrum. The resolution is 1.0 cm⁻¹.

dimers complicate the picture even more, and finally, if H₂O₂ is present in large quantities, there is also a contribution from its $\nu_2 + \nu_6$ combination band, which by accident falls in the same region. Some of the peaks are also fairly broad, so that even better resolution does not help. Due to these difficulties, the assignments in this region are less certain than the others. The peaks which are given in Tables 1–3 are assigned by comparing several spectra which all contain different relative amounts of HDO₂ and D₂O₂.

4. Discussion

According to our knowledge this is the first time the gaseous products of the thermal decomposition of UHP are directly measured. FTIR technique allows one to detect the temperature at which the sample starts to decompose and thus to define the useful temperature range for obtaining only hydrogen peroxide from the parent molecule. According to our results the upper limit is 92 °C. Because we did not monitor gases directly generated in the sample chamber (see Experimental Section), this temperature value is probably slightly overestimated.

The main product below 92 °C is hydrogen peroxide, water being only barely visible in the spectrum. O₂ cannot be detected by IR spectroscopy, but its concentration must follow the

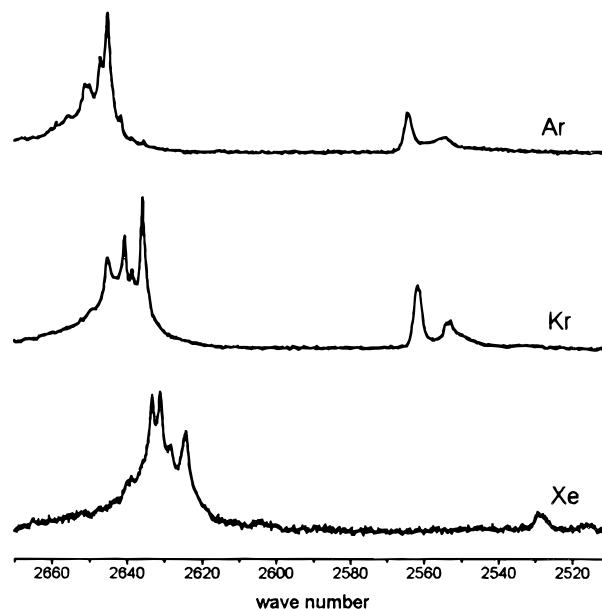


Figure 7. OD stretching region of matrix-isolated HDO₂ and D₂O₂. The resolution is 0.25 cm⁻¹.

concentration of water because they are connected by the dissociation reaction of hydrogen peroxide. In any case, O₂ may also be present in our samples in small amounts as an impurity. However, this should not be a significant problem in matrix studies because our results do not show significant complexation of H₂O₂ even with water. In a matrix with a very high water concentration, we observed additional peaks, which were most probably due to the water hydrogen peroxide complex. In other cases the concentration of water could be kept sufficiently low to avoid complex formation. The decomposition of H₂O₂ could probably be suppressed even more by using only plastic parts in the system in order to avoid catalytic decomposition at the surfaces.

Hydrogen peroxide belongs to a point group C_2 . The potential function with respect to internal rotation is characterized by a higher energy *cis* barrier and a lower energy *trans* barrier.³¹ The *trans* tunneling splits the torsional energy levels, which are characterized by quantum numbers n and τ .³¹ The quantum number n takes values 0, 1, 2, 3, ... and the *trans* tunneling splits the degenerate τ levels into two groups of levels with $\tau = 1, 2$, and $\tau = 3, 4$. This results in energy levels labeled ($n = 0; \tau = 1, 2$), ($n = 0; \tau = 3, 4$), ($n = 1, \tau = 1, 2$), ($n = 1; \tau = 3, 4$), etc. in the order of increasing energy. The selection rules for hydrogen peroxide when both *cis* and *trans* tunneling are taken into account are given by Hougen.³² For ν_1 , ν_2 , and ν_3 , transitions between the levels with $\tau = 1, 2 \leftrightarrow \tau = 3, 4$ are allowed, and for ν_5 and ν_6 , transitions between the levels with $\tau = 1, 2 \leftrightarrow \tau = 1, 2$ and $\tau = 3, 4 \leftrightarrow \tau = 3, 4$ are allowed.³²

The consequence of this is that the IR spectrum of hydrogen peroxide consists of doublets. The extent of the splitting is, however, different for different vibrational states, and especially in the solid state environment it is further modified by intermolecular forces, and therefore, it is not obvious that we should always observe two separate peaks. At very low temperatures, transitions from the first excited state should be weak because of the reduced population. In the gas phase the separation of the ground state and the first excited state is 11.44 cm⁻¹.¹⁵ Applying the Boltzmann distribution to this value gives the intensity ratio of about 1:3 at 15 K, which is in a good qualitative agreement with the intensity ratio of the observed doublet of ν_6 (see the argon spectrum in Figure 4).

The OH stretching region of H₂O₂ is less thoroughly studied^{14,16} than, for example, the OH bending region,^{15,17,18} probably partly because of the difficulties due to overlapping of ν_1 and ν_5 and the interference of water bands. According to Olson et al.,¹⁶ the band centers of the two components of ν_5 lie at 3610.66 and at 3618.84 cm⁻¹. For ν_1 Olson et al. give more tentative values of 3609.8 and 3617.95 cm⁻¹. In argon, we observe two peaks at 3597.0 and 3587.8 cm⁻¹ in accordance with Lannon et al.²⁰ who assigned these peaks to ν_5 and ν_1 , respectively. We reassign them to the two components of ν_5 with some contribution from the overlapping ν_1 peaks, which according to Olson et al.¹⁶ should be much weaker than ν_5 peaks.

In the bending region, the two peaks at 1277.0 and 1270.9 cm⁻¹ must belong to the monomer because both of them are present in the most diluted samples in which the strong multimer peaks cannot be detected in the stretching region. Lannon et al.²⁰ assigned the lower wave number peak to ν_6 and the higher wave number peak to the symmetric bending ν_2 . In the gas phase, the ν_2 Raman value is 1393.5 cm⁻¹,³³ suggesting, according to the assignment of Lannon et al., an unlikely red shift of more than 100 cm⁻¹ when going from the gas phase to argon matrix. We therefore assign these peaks to two double-minimum components of the antisymmetric bending mode ν_6 . The splitting (6.1 cm⁻¹) is similar to the gas phase value¹⁵ of 9.1 cm⁻¹, and the difference can be explained by the interactions between H₂O₂ and the solid host. In krypton and xenon matrices the splitting is further reduced to 5.0 and 4.6 cm⁻¹, respectively. The splitting in the OH bending of HOOD can also be seen, and the corresponding values are 7.7, 6.8, and 5.2 cm⁻¹ in argon, krypton, and xenon, respectively. We could not resolve any doublet structure in OD bending mode peaks either in HDO₂ or in D₂O₂ even with a resolution of 0.25 cm⁻¹.

The observed weak peak at 1417.9 cm⁻¹ in argon is assigned to the symmetric bending ν_2 of a multimer. The same wave number has been reported by Kuo et al.²² in a table among many other values, but it is not assigned. The shift of 24.4 cm⁻¹ from the gas phase monomeric Raman value is reasonable for the associated form. Giguere and Srinivasan³⁴ observed in their Raman measurements of argon-matrix-isolated H₂O₂ a peak at 1385 cm⁻¹, which they assigned to ν_2 . No indication of absorptions at 1385 cm⁻¹ was found in the present study even with the highest concentrations of hydrogen peroxide indicating the weakness of monomeric ν_2 .

A weak absorption at 2643.6 cm⁻¹ with a smaller component at 2653.0 cm⁻¹ are assigned to the two components of the combination mode $\nu_2 + \nu_6$ of the monomer. Our values are quite near the gas phase band origins at 2649.01 and 2660.71 cm⁻¹.¹⁵ Finally the very weak O—O stretching fundamental is found at 865.6 cm⁻¹, which is near the 869 cm⁻¹ Raman peak of Giguere and Srinivasan.³⁴ Our peak, however, belongs to a multimer and the corresponding absorption could not be seen in monomeric matrices.

A few other peaks are visible especially in the most concentrated samples and these are assigned to multimers without further definition of the species. These wave numbers are included in Tables 1–3. It is to be noted, however, that according to the two recent ab initio studies the cyclic dimer should be the most stable form of the dimer.^{35,36} In Kr and Xe matrices, the spectrum of H₂O₂ is very similar to that in argon, and the observed wave numbers are given in Tables 1–3.

The spectrum of D₂O₂ is analogous to H₂O₂ and the absorptions are given in Tables 1–3. The partially deuterated species HDO₂ provides some interesting details. Because it is unsymmetrical, both the OH and OD bending modes possess strong IR intensity (see Figures 5 and 6). The OH bending

shows a clear doublet structure. In argon, the bending absorptions lie at 1350.3 and 1342.6 (OH doublet) and at 980.9 cm⁻¹ (OD bending), respectively. The OH and OD stretching absorptions are overlapped with those of H₂O₂ and D₂O₂, which are both present in matrices where HOOD is observed. This makes the assignments of ν_{OH} and ν_{OD} for HDO₂ and D₂O₂ difficult, as mentioned previously. Finally, the multimer peaks in deuterated matrices are complicated by the possibility of all possible combinations of different isotopomers.

5. Conclusions

We have studied the gaseous products emitted from the thermal decomposition of urea hydrogen peroxide (UHP). The results show that below ~90 °C only hydrogen peroxide is emitted and after that urea starts to decompose. Furthermore, it was observed that in an argon flow H₂O₂ is not decomposed significantly.

By taking advantage of the results obtained from the gas phase studies, we have used UHP as a source of hydrogen peroxide for matrix isolation experiments. The IR spectra of different isotopomers of hydrogen peroxide in argon, krypton, and xenon matrices are presented including the first rare gas matrix IR value for $\nu_2 + \nu_6$. Splitting of several bands is attributed to the effects due to the double minimum with respect to internal rotation in H₂O₂. Experiments in argon are compared with the previous results. The IR spectra of hydrogen peroxide in krypton and xenon matrices are reported for the first time.

Acknowledgment. This work was partially supported by the EU project LAMOCS, Grant ENV4-CT95-0046. We gratefully acknowledge Temet Instruments, Inc., for providing us with the Gasmet FTIR—gas analyzer. We thank Dr. Tarja Laitalainen for kindly providing the sample of urea hydrogen peroxide in the beginning of this research.

References and Notes

- (1) For example, see: Wayne, R. P. *Chemistry of Atmospheres*, 2nd ed.; Clarendon Press: Oxford, 1991; Chapter 5.
- (2) Cooper, M. S.; Heaney, H.; Newbold, A. J.; Sanderson, W. R. *Synlett* **1990**, 533.
- (3) Ondrey, G.; van Veen, N.; Bersohn, R. *J. Chem. Phys.* **1983**, *78*, 3732.
- (4) Docker, M. P.; Hodgson, A.; Simons, J. P. *Chem. Phys. Lett.* **1986**, *128*, 264.
- (5) Gericke, K.-H.; Klee, S.; Comes, F. J.; Dixon, R. N. *J. Chem. Phys.* **1986**, *85*, 4463.
- (6) Klee, S.; Gericke, K. H.; Comes, F. J. *J. Chem. Phys.* **1986**, *85*, 40.
- (7) Klee, S.; Gericke, K. H.; Comes, F. J. *Ber. Bunsen-Ges. Phys. Chem.* **1988**, *92*, 429.
- (8) Zhang, D. H.; Zhang, J. Z. *J. Chem. Phys.* **1993**, *98*, 6276.
- (9) Satterfield, C. N.; Kavanagh, G. M.; Resnick, H. *Ind. Eng. Chem.* **1951**, *43*, 2507.
- (10) Heaney, H. *Aldrichimica. Acta* **1993**, *26*, 35.
- (11) Lorant, B. *Seifen, Oele, Fette, Wachse* **1966**, *92*, 644.
- (12) Ball, M. C.; Massey, S. *Thermochim. Acta* **1995**, *261*, 95.
- (13) Giguère, P. *J. Chem. Phys.* **1949**, *18*, 88.
- (14) Redington, R. L.; Olson, W. B.; Cross, P. C. *J. Chem. Phys.* **1961**, *36*, 1311.
- (15) Hillman, J. J.; Jennings, D. E.; Olson, W. B.; Goldman, A. *J. Mol. Spectrosc.* **1986**, *117*, 46.
- (16) Olson, W. B.; Hunt, R. H.; Young, B. W.; Maki, A. G.; Brault J. W. *J. Mol. Spectrosc.* **1988**, *127*, 12.
- (17) Perrin A.; Flaud, J.-M.; Camy-Peyret, C. *J. Mol. Spectrosc.* **1990**, *142*, 129.
- (18) Perrin, A.; Valentin, A.; Flaud, J.-M.; Camy-Peyret, C.; Schriver, L.; Schriver, A.; Arcas, Ph. *J. Mol. Spectrosc.* **1995**, *171*, 358.
- (19) Catalano, E.; Sanborn, R. *J. Chem. Phys.* **1963**, *38*, 2273.
- (20) Lannon, J. A.; Verderame, F. D.; Anderson, R. W., Jr. *J. Chem. Phys.* **1971**, *54*, 2212.
- (21) Tso, T.-L.; Lee, K. C. *J. Phys. Chem.* **1985**, *89*, 1612.

- (22) Kuo, Y-P.; Wann, G-H.; Lee, Y-P. *J. Chem. Phys.* **1993**, *99*, 3272.
- (23) Lehto, J.; Pettersson, M.; Hinkula, J.; Räsänen, M.; Elomaa, M. *Thermochim. Acta* **1995**, *265*, 25.
- (24) Saarinen, P.; Kauppinen, J. *Appl. Spectrosc.* **1991**, *45*, 953.
- (25) Elvers, B.; Hawkins, S.; Ravenscroft, M.; Schultz, G. *Ullmans Encyclopedia of Industrial Chemistry*, 5th ed.; VCH Verlagsgesellschaft mbH: Weinheim, 1989; Vol. A13, p 462.
- (26) Lu, C-S.; Hughes, E. W.; Giguère, P. A. *J. Am. Chem. Soc.* **1941**, *63*, 1507.
- (27) Greenwood, N. N.; Earnshaw, A. *Chemistry of the Elements*, 1st ed.; Pergamon Press: Oxford, 1994; p 343.
- (28) Herzberg, G.; Reid, C. *Discuss. Farad. Soc.* **1950**, *9*, 92.
- (29) Engdahl, A.; Nelander, B. *J. Mol. Struct.* **1989**, *193*, 101 and references therein.
- (30) Andrews, L.; Davis, S. R. *J. Chem. Phys.* **1985**, *83*, 4983.
- (31) Hunt, R. H.; Leacock, R. A.; Peters, C. W.; Hecht, K. T. *J. Chem. Phys.* **1965**, *42*, 1931.
- (32) Hougen, J. T. *Can. J. Phys.* **1984**, *62*, 1392.
- (33) Giguère, P. A.; Srinivasan, T. K. *J. Raman Spectrosc.* **1974**, *2*, 125.
- (34) Giguère, P. A.; Srinivasan, T. K. *Chem. Phys. Lett.* **1975**, *33*, 479.
- (35) Dobado, J. A.; Molina, J. M. *J. Phys. Chem.* **1993**, *97*, 7499.
- (36) Mo, O.; Yanez, M.; Rozas, I.; Elguero, J. *J. Chem. Phys.* **1994**, *100*, 2871.